Earthq Sci (2016) 29(3):173–184
DOI 10.1007/s11589-016-0153-4

RESEARCH PAPER

Active faults and seismogenic models for the Urumqi city, Xinjiang Autonomous Region, China

Yingzhen Li · Yang Yu · Jun Shen · Bo Shao · Gao Qi · Mei Deng

Received: 8 October 2015 / Accepted: 9 May 2016 / Published online: 28 June 2016

Abstract We have studied the characteristics of the active faults and seismicity in the vicinity of Urumqi city, the capital of Xinjiang Autonomous Region, China, and have proposed a seismogenic model for the assessment of earthquake hazard in this area. Our work is based on an integrated analysis of data from investigations of active faults at the surface, deep seismic reflection soundings, seismic profiles from petroleum exploration, observations of temporal seismic stations, and the precise location of small earthquakes. We have made a comparative study of typical seismogenic structures in the frontal area of the North Tianshan Mountains, where Urumqi city is situated, and have revealed the primary features of the thrust-fold-nappe structure there. We suggest that Urumqi city is comprised two zones of seismotectonics which are interpreted as thrust-nappe structures. The first is the thrust nappe of the North Tianshan Mountains in the west, consisting of the lower (root) thrust fault, middle detachment, and upper fold-uplift at the front. Faults active in the Pleistocene are present in the lower and upper parts of this structure, and the detachment in the middle spreads toward the north. In the future, *M*7 earthquakes may occur at the root thrust fault, while the seismic risk of frontal fold-uplift at the front will not exceed *M*6.5. The second structure is the western flank of the arc-like Bogda nappe in the east, which is also comprised a root thrust fault, middle detachment, and upper fold-uplift at the front, of which the nappe stretches toward the north; several active faults are also developed in it. The fault active in the Holocene is called the South Fukang fault. It is not in the urban area of Urumqi city. The other three faults are located in the urban area and were active in the late Pleistocene. In these cases, this section of the nappe structure near the city has an earthquake risk of *M*6.5–7. An earthquake M_S6.6, 60 km east to Urumqi city occurred along the structure in 1965.

Keywords Urumqi · Active fault · Seismogenic structure · Thrust · Nappe

Y. Li · Y. Yu (✉) · J. Shen · B. Shao · G. Qi · M. Deng
Institute of Disaster Prevention, Beijing 101601, China
e-mail: yuyang_eq@126.com

1 Introduction

To achieve earthquake prevention and disaster reduction, extensive investigations of active faults and assessment of seismic hazards are currently under way in city areas across the Chinese mainland. For this work, one of the vital steps is to establish a proper seismogenic model in agreement with local tectonic features. This requires an integrated analysis of investigations in the shallow and deep subsurface, as well as an understanding of the relationship between shallow and deep structures and tectonic evolution processes. For instance, steeply dipping strike-slip faults exhibit the same geometry on the surface and at depth, whereas for low-angle thrust fault-fold structures, what is seen on the ground is inconsistent with the seismogenic pattern at depth.

Since the 1980s, geologists have noticed that some major earthquakes are associated with buried thrust-fold structures (Stein and Yeats 1989), such as the 1980 El Asnam, Algeria; 1983 Coloinga, USA (Stein 1984); 1985 Kettleman, USA; and 1987 White Narrow, USA earthquakes. The 1906 Manas, North Tianshan, Xinjiang great earthquake is also attributed to a thrust-fold structure (Zhang et al. 1994), which consists of a deep fault at the southern margin of the Junggar basin, detachment in the

crust and a fault-ramp in the shallow subsurface at Manas (Wang et al. 2001).

Urumqi city lies in the Cenozoic fold zone in front of the North Tianshan Mountains. Before the Late Paleozoic, the territory of modern Tianshan Mountains is a part of Paleo-Asian ocean (Khain et al. 2003), remaining mainly in a relatively stable level of subsidence. At the end of the Late Paleozoic, the Paleo-Asian ocean began to close. The area of Tianshan Mountains transformed into an island-arc tectonic environment with frequent activity (Burbank and Anderson 2001). In the Late Permian, the collision history ended and uplifting began, and the strata of Paleozoic-folded leading to the foundation of the modern Tianshan Mountains. Tectonic movement was small in scale during the Mesozoic and early of Cenozoic. At the end of Eogene, most areas were denudation and planation, forming a regional planation surface. In Eocene-Oligocene period in Paleogene, the collision between the Indian plate and the Eurasian plate made the Ancient Tianshan folding belt of Paleozoic and Mesozoic tectonic resurrect, leading to the further new uplifting of the mountain again and the basins on both sides sinking, forming modern topography and structural framework gradually (Deng et al. 2000).

The study area is the central section of northern Chinese Tianshan and south of Junggar basin. the chaiwopu basin is in the south, the Junggar basin is in the north, and in the middle is the Xishan fault-bounded uplift which is the eastward prolongation of the Changji-Kalaza anticline. Influenced by the arc-like Bogda nappe structure, the strike of the axis of the anticline turns from WNW in the west to nearly E-W in the east.

The strata in the study area include layers deposited from Devonian of Paleozoic to Quaternary. Paleozoic is composed of marine sediments. The Mesozoic and Cenozoic are composed of continental sediments. Most of the Devonian strata are limestone, calcareous sandstone, and andesite. The Carboniferous strata mainly consist of volcano tuff, silty mudstone, and valley-stone. The Permian strata consist of feldspar sandstone, feldspar quartz sandstone, oil shale, calcareous sandstone, and silty mudstone. Triassic strata consist of mid-thick-layered mudstone, sandy mudstone, thick-layered hard sandstone, and calcareous mudstone. Jurassic consists mainly of conglomerate, sandstone, sandy mudstone, silty mudstone, and coal seam. The Cretaceous strata consist of mudstone, sandstone, and conglomerate. Eogene strata consist of mudstone and sandstone. Neogene strata consist of sandy conglomerate, sandstone, and sandy mudstone. Most of Quaternary strata consist of alluvial deposit, fluvial gravel, and sand layers (Song et al. 2009).

Cenozoic tectonic deformation of the Tianshan is characterized by expansion to the north and south sides in the meantime and development of reverse fault and fold belts (Avouac et al. 1993; Liu et al. 1994; Zhang et al. 1996; Abdrakhmatov et al. 1996; Ghose et al. 1998; Allen et al. 1999; Burbank et al. 1999; Burchfiel et al. 1999; Deng et al. 2000; Fu et al. 2003). These nappe structures developed in Quaternary are of the most intense regions of tectonic deformation, and the strongest earthquakes have occurred along these structures (Yang et al. 2008; Wu et al. 2011, 2016).

The slip rate of southern boundary fault of Junggar basin is estimated with GPS observation data as about 5.6 ± 1.0 mm/a (Li et al. 2016). It is close to the shortening rate of northern Tianshan, estimated with geologic data, as 2–9 mm/a in Holocene (Avouac et al. 1993; Burchfiel et al. 1999; Deng et al. 2000).

The thrust-fold structure zone in front of the North Tianshan Mountains can be divided into three sections (Kuang and Qi 2006; Li et al. 2006): in the west, the Tuositai nappe, dominated by the Sikeshu depression; in the east, an arc-shaped thrust in front of Bogda with the Fukang fault, and in the intervening middle section, the range-frontal nappe of the North Tianshan. In the N-S (longitudinal) direction, these structures comprise three rows of structures. The first one is also called the range-frontal fold zone as a result of the Yanshan movement, the second is the anticline in the depression largely in the Paleogene System, and the third is the anticline at the edge of the depression mainly in the Neogene System. As a whole, deformation of the thrust-fold structures spreads from the mountains in the south to the basin in the north. The Bogda nappe can also be divided into three sections. The first one, south to the North Bogda fault, is the nappe made up of the Bogda Mountains of the Carboniferous System. The second, between the Yamalik fault and the Bogda fault, is the first wedge-like detachment of the Permian System, and the third one is the second detachment wedge of the Triassic and Jurassic Systems south to the Bogda fault and north to the Yamalik fault. In the footwall of the Fukang fault in the north, the cover of upper Permian and Quaternary Systems exhibits weak deformation (Wang and Shen 2000; Wu and Guo 1991).

Urumqi city is situated at the intersection of the middle section of the range-frontal thrust of the North Tianshan Mountains and its eastern section, arcuate thrust in front of the Bogda Mountains (Fig. 1). This position also corresponds to the western end of the first row of the North Tianshan range-frontal anticline zone, and the western flank of the second and third rows of the thrust zone in the Bogda reverse fault-fold structure.

2 Surface active faults of Urumqi city

Geological investigations show that the surface active faults strike in E-W, ENE, and NE directions, dipping toward the north and south. The faults southward dipping

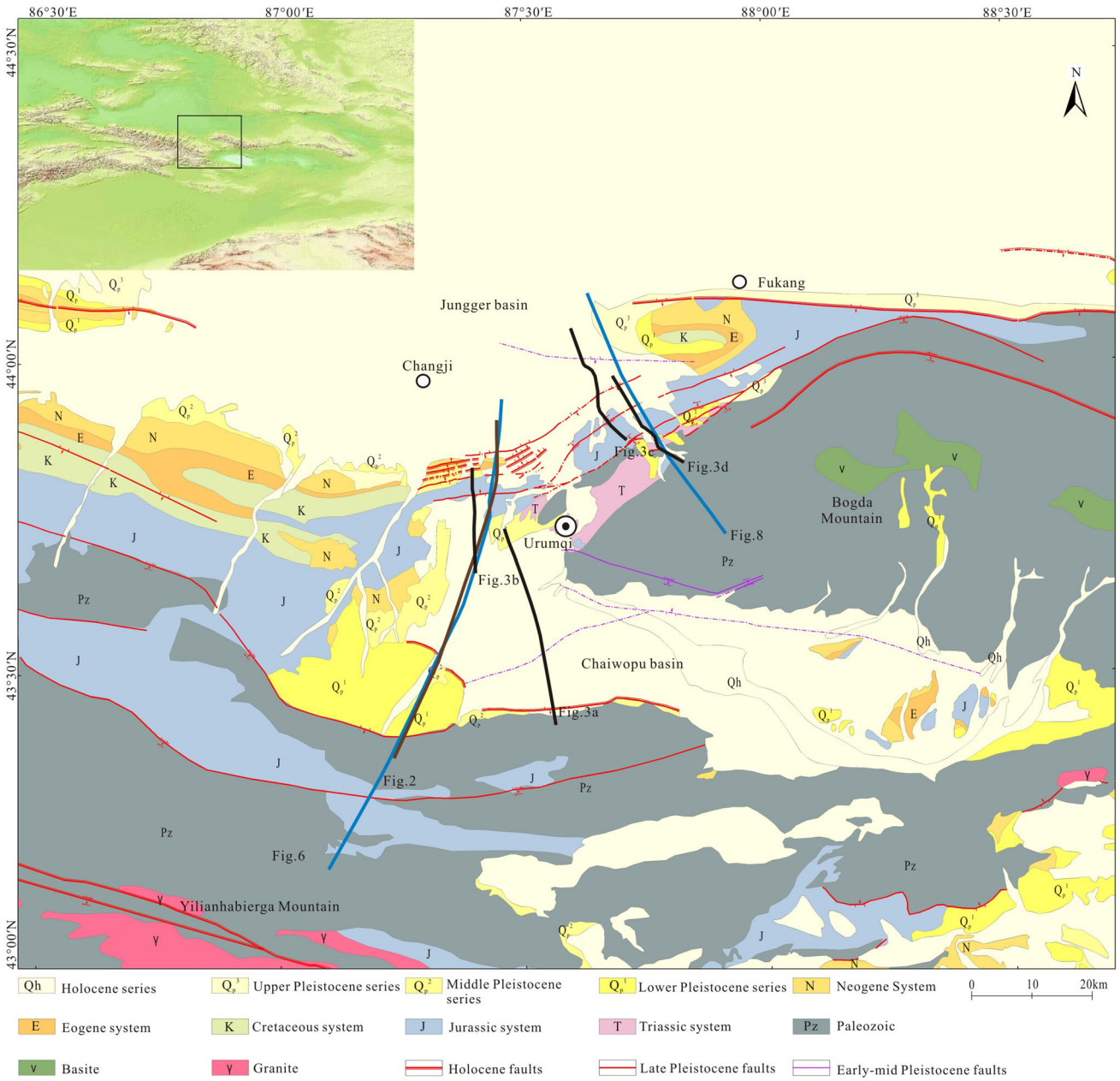

Fig. 1 Tomography in the vicinity of Urumqi city. The *black square* outlines the urban area of Urumqi city, the *brown line* is the position of the deep seismic reflection profile, the *black lines* are the positions of the petroleum seismic reflection profiles, and the *blue lines mark* the positions of the seismotectonic model profiles

include the Yamalik fault and Bagang-Shihua hidden fault, between which are north-vergent faults such as the Wanyaogou and Baiyangnangou faults east to the Urumqi River, and the Xishan fault, Wangjiagou fault set and Jiujiawan fault set west to the Urumqi River. Among them, the Jiujiawan fault set is of normal type and the others are reverse faults. In general, these faults become younger in age of activity from south to north. The Xishan, Wanyaogou, Baiyangnan, and Bagang-Shihua faults were active in the late Pleistocene, with no further offsets since the Holocene. There is no evidence of displacement on the Yamalik fault in the late Pleistocene strata; thus, it was active before the middle Pleistocene. To the east, near the apex of the Bogda arc, the Baiyanggou fault might have been active since the Holocene, while to the west, in Urumqi city, it was only active in the late Pleistocene. Both the Wangjiagou fault set and Jiujiawan fault set have been active since the Holocene.

3 Deep structures

3.1 Deep seismic sounding profile

The Center for Geophysical Exploration, China Earthquake Administration, has completed a deep seismic sounding profile through Urumqi city (brown line in Fig. 1). In the south, it commences at the front of the North Tianshan, extending northwards across the chaiwopu basin and Xishan range, and ends in the Junggar basin in the north, totaling 78 km in length.

The P wave velocity model is established for time-depth conversion of the deep seismic reflection profile (Liu et al. 2007). The shallow part of the model is obtained from the travel time curve by shallow seismic refraction survey. The middle-deep part is obtained by the stacking velocity data acquired from the processing of the deep seismic reflection data, via the DIX equation (Chen et al. 2012). The deep part is obtained from the wide-angle reflection detection in the study area (Deng et al. 2000).

On the CDP stack cross-section, there are many dense reflections above the two-way travel time (TWT) of 5 s, which reveal the relief of the interfaces. Bounded by Xishan, they exhibit different features of the subsurface structures (Fig. 2). South to Xishan, the reflections are associated with several rows of thrust-anticlines in an E-W direction, which are steep at shallow levels and gentle in the deep subsurface. Around Xishan and Wangjiagou (station 45–55 km), the reflections are generated by steep northward-dipping strata which accord with the Xishan and Wangjiagou fault set on the surface.

North to station 55 km, the seismic reflection profile indicates a set of flat strata that has dense and laterally continuous reflections. It characterizes a typical sedimentary basin with a greatest depth of 10–12 km.

South to station 45 km, a set of tilt reflective events R_A with strong energy is very obvious. It appears at TWT 6.6 s at the southern end of the profile, corresponding to a depth of 17–18 km. Toward the north along the profile, this reflective horizon gets gradually shallower, and is at a depth of 10 km near station 43 km. In fact, it is the low-angle thrust fault, or detachment, below the front of the North Tianshan to the Xishan range.

The deep seismic reflection profile reveals that there are 10 distinct faults above the detachment. Fault F_1 lies near station 7.5 km, of which the north side has different reflections and interface occurrences. Fault F_2 at station 17 km is also clear on the profile. Both faults have been active since the Holocene and are visible on the ground. Near Xishan farm (station 35 km), fault F_3 is hidden in the subsurface, which should be the trace of the buried fault on the northern edge of the chaiwopu basin. On the profile, the strata have a steep dip angle in the hanging wall of fault F_3 and a gentle dip angle in the footwall. Around station 42 km is the branch of the Yamalik fault (F_4), above which the strata become gently dipping from shallow to deep subsurface. Fault F_5 lies beneath the Yamlik fault and merges with the reflective zone R_A downward at a depth of 10 km. In a general view, faults F_1–F_5 and reflective zone R_A constitute a complete listric thrust system on the profile as well as a thrust block in the upper crust, wherein R_A serves as a decollement.

The profile section from station 45–55 km runs across the Xishan fault (F_6) and Wangjiagou fault set (F_7–F_{10}). Because of exposed basal rocks in this section, steep strata and northward-dipping faults can be seen at the surface. The deep seismic reflection profile also shows that F_6–F_{10} all dip toward the north, of which the fault planes are steep in the shallow subsurface and gentle in the deep subsurface, in agreement with what is seen on the ground, both spatially and structurally. The faults F_6 and F_{10} are the southern and northern boundaries of the block, respectively, between which there is a set of steeply northward-dipping reflections, which are interpreted as the interlayer faults due to compression, i.e., faults F_7, F_8, and F_9. These faults appear at the near surface and terminate at a depth of 10 km.

Between the Xishan and Yamalik faults is a compressive triangular area. By comparison with the seismic survey from petroleum exploration, it can be inferred that the Xishan anticline or fault-bounded uplift (the eastward prolongation of the Kalaza anticline) is the result of incorporation of the frontal edge and counter-reverse fault in a large-scale fold (Li et al. 2004). It is a pop-up or triangular zone structure characterized by strong deformation. In addition to F_5, there are probably reverse faults and thrust sheets of lower angles below the block, which stack to thicken the crust, thus causing range of the Xishan fault-bounded block (Ran et al. 2007).

At TWT 9–10 s, there is a reflective lamination zone R_B very gently dipping to the south (Fig. 2). It is 27-km deep (TWT 9 s) at the northern end of the profile and 31-km deep (TWT 10.5 s) at the southern end, respectively. As the reflective features above and below this lamination zone are completely different, it should be the boundary between the upper crust and the lower crust. The lower crust, TWT 10–14 s, has a relatively simple and more transparent structure without folded laminations.

The reflective zone R_C on the profile, as a set of small-sized, nearly parallel laminations, is the crust-mantle transition. Its upper boundary appears at TWT 14.5 s at the southern end of the profile, equivalent to a depth of 45 km, and it lies at TWT 13.8 s at the northern end corresponding to a depth of 42.8 km. In the vertical direction, this zone

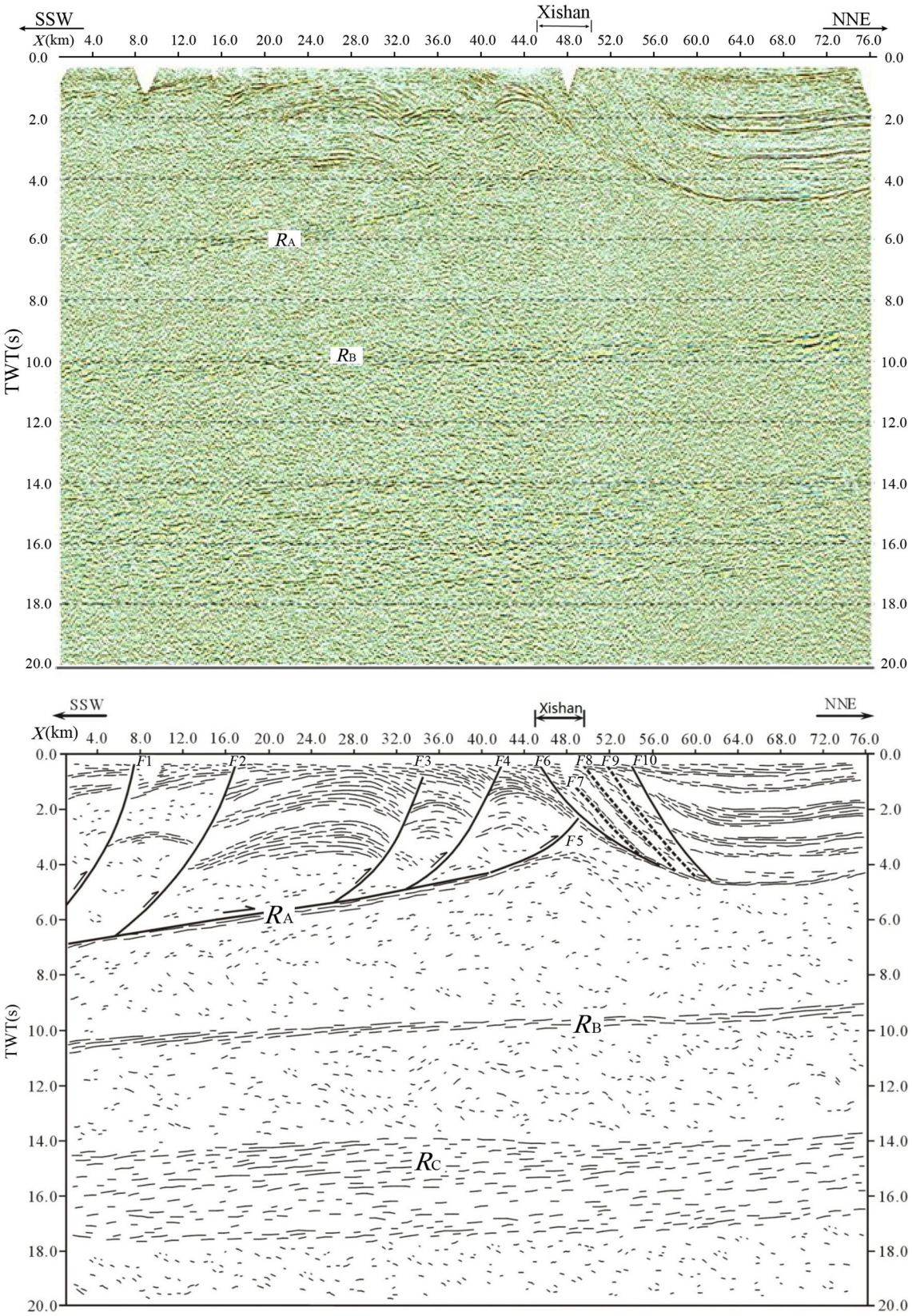

Fig. 2 Deep seismic reflection profile (for location, see Fig. 1)

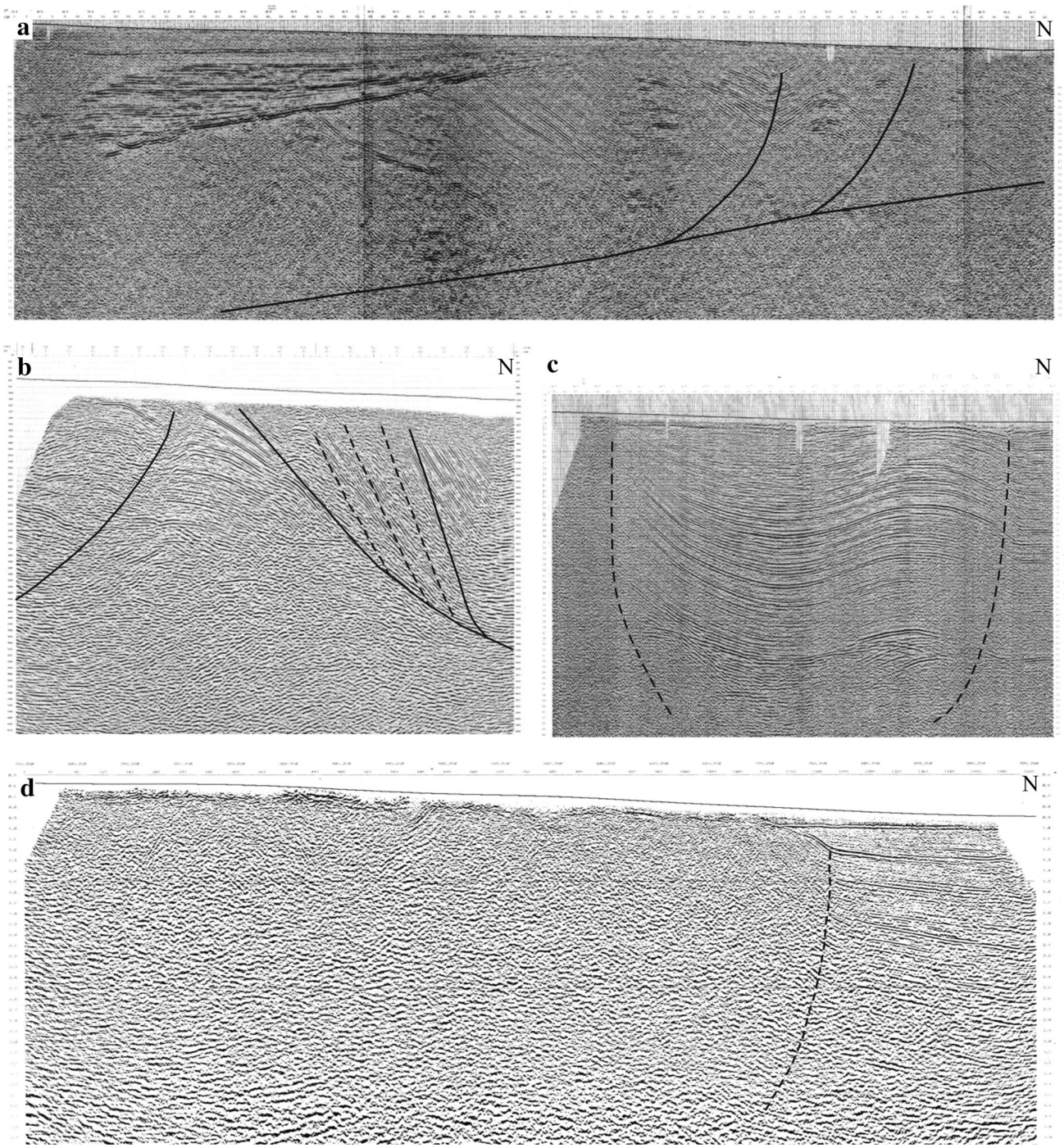

Fig. 3 Petroleum seismic reflection profile surrounding Urumqi city (for locations, see Fig. 1)

spans some 3 s of TWT, implying a thickness of 9–10 km, of which the lower boundary is the Moho at a depth of 52–55 km, dipping slightly to the south.

3.2 Seismic profiles from petroleum exploration

This work by the Xinjiang Oilfield Company, China National Petroleum Corporation (CNPC) produced four seismic profiles. There are two seismic profiles on each side of the Urumqi River (see Fig. 1 for their locations). The two profiles in the west are close to the deep seismic sounding profile presented in the previous section and reveal similar structures in the upper portion (above TWT 6 s) with a higher resolution. They include the monocline and fault structures beneath the Xishan range (Fig. 3b), and complex-folded strata and faults between Xishan and Yamalik Mountains

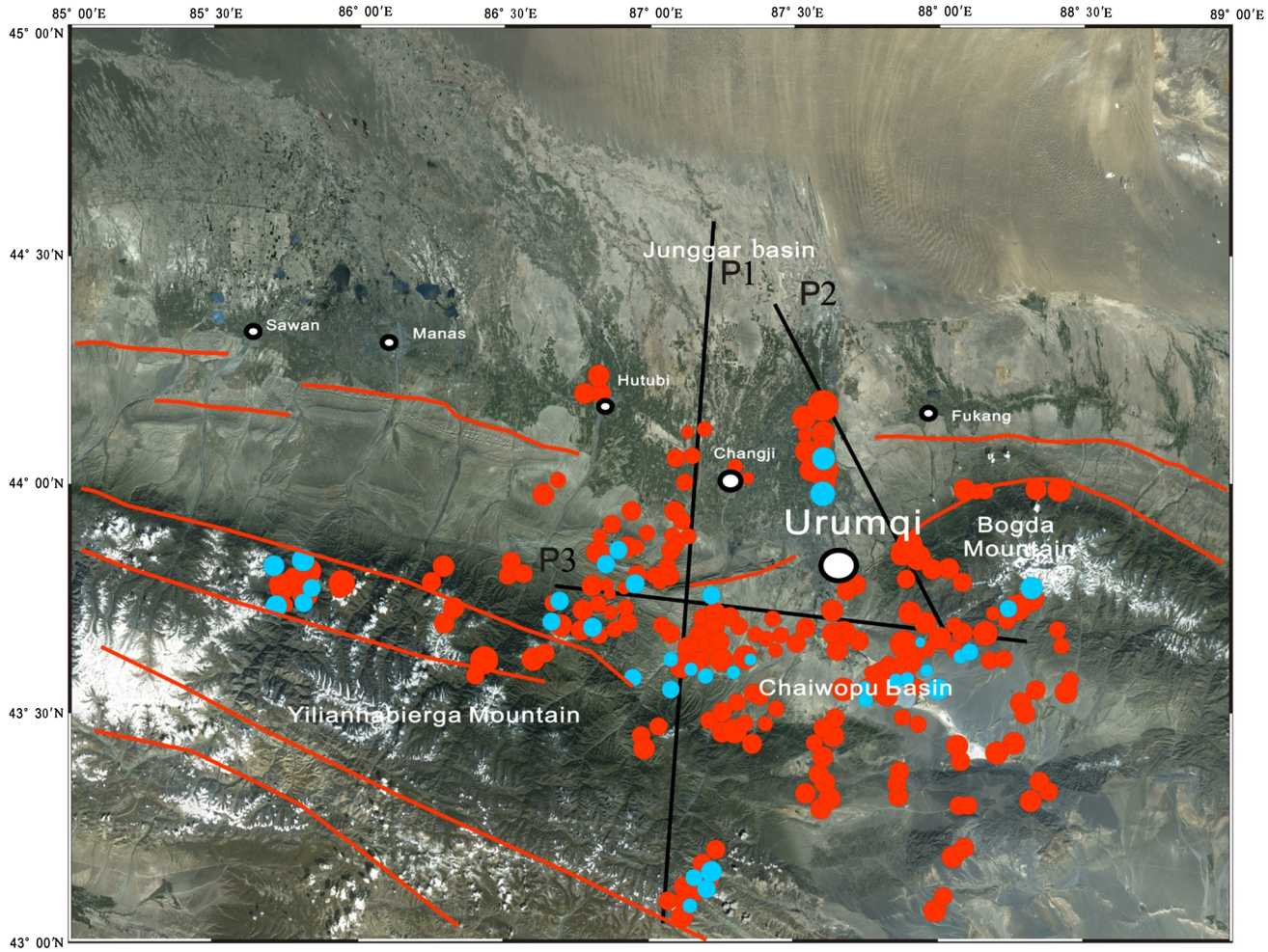

Fig. 4 Distribution of epicenters in 2004.8.2–2005.8.10 observed by a floating seismic array surrounding Urumqi city and located by the Hypoinverse and HypoDD methods. *Red circles* are the epicenters located by the HypoDD method, *blue circles* are located by the Hypoinverse method

(Fig. 3a). The other two profiles in the east cross the western portion of the Bogda arc. Figure 3d shows a large difference of type of sediments on the opposite side of the Bagang-Shihua fault, meaning that this fault is the boundary between the nearly E-W trending uplift and the Junggar basin in the middle of Urumqi city. Figure 3c also indicates such a difference, as well as the broad-gentle folds of the Gumudi anticline north to the Bagang-Shihua fault in the southern Junggar basin and thrust faults in the south, which are the Fugkang-south fault seen at the surface and the hidden Dachaotan fault. In summary, these profiles demonstrate that thrust faults and folds characterize the deep structures in the Urumqi city area.

4 Precise relocation of small earthquakes

For this work, 10 broadband seismometers were operated for one year (2 August 2004–10 August 2005) in Urumqi city and recorded many small earthquakes in this region. In total, 727 events were initially located, on average with square root residual 0.77 s of seismic phase, epicenter error 1.4–4.5 km, and focal error 3.3–10.4 km. After relocation by the Hypoinverse and double-difference method, these errors were reduced to 0.67 s, 2.9–3.4 km, and 4.7 km, respectively.

As shown in Fig. 4, these newly recorded small earthquakes are primarily distributed in the perimeter of the chaiwopu basin in the south, the range-front of the North Tianshan in the west, and the Bogda Mountains and southern Junggar basin in the east. They are associated with active faults in these areas, such as those on the northern and southern margins of the chaiwopu basin, the Erdaogou fault in the Bogda Mountains, Fukang fault in the southern edge of the Junggar basin, and faults along the Kalaza anticline and Qigu anticline in the west. A few events have been recorded within Urumqi city in the year of the observations.

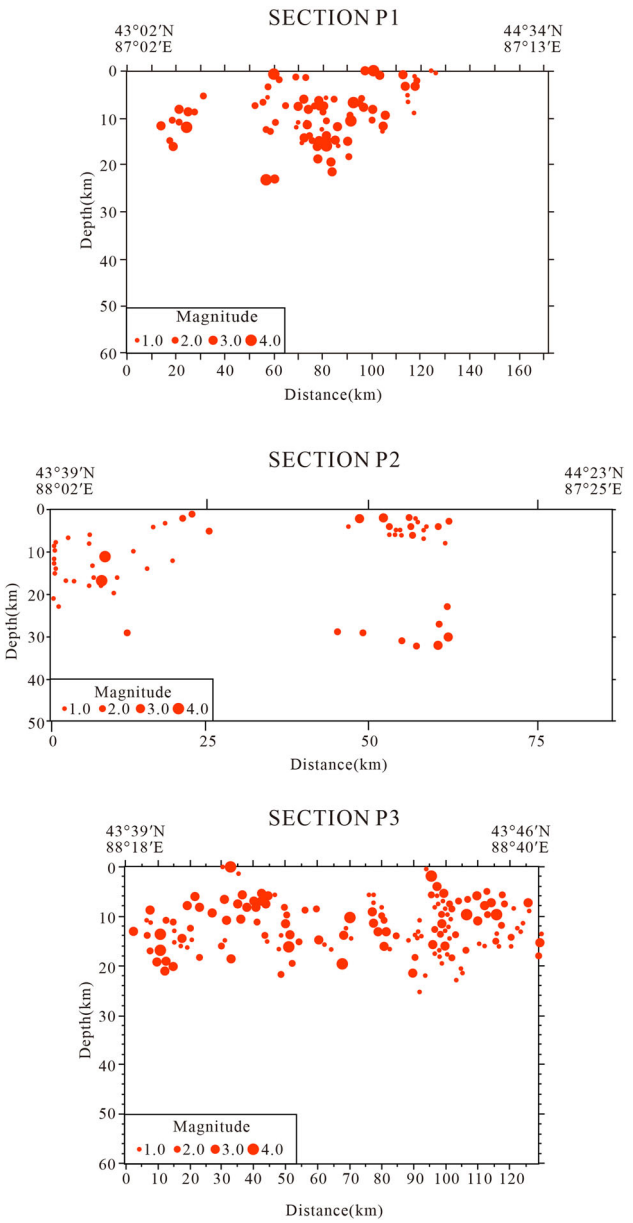

Fig. 5 Hypocenter depths of the earthquakes within 20 km of lines P1-P3 in Fig. 4

Figure 5 displays the projections of focal depths of the small events on three profiles P_1-P_3. They demonstrate that most earthquakes occurred at depths of 15–18 km, consistent with the position of the detachment revealed by seismic reflection profiles.

5 Seismogenic models

Based on analysis of the relationship between active faults and seismotectonics, Urumqi city is associated with two seismogenic structures (Yeats 1986); one is to the west of the Urumqi River and the other is to the east. In the west, the seismogenic structure is analogous to that of the *M*7.7 event south of Manas in 1906, associated with the range-frontal thrust skin structure in the Yilianhabierga Mountains, and called the North Tianshan range-frontal seismogenic structure. In the east, it is named the Bogada-arc west flank seismogenic structure.

5.1 North Tianshan range-frontal seismogenic structure

By integration of data from the deep seismic soundings, petroleum seismic reflection surveys, relocation of small earthquakes, and geological investigations, we have established a seismogenic model for western Urumqi city (Fig. 6).

It is a typical thrust surface structure made up of three zones. The southern zone is the fault belt in front of the North Tianshan or the southern edge of the Chaiwopu basin, which is the root portion of the surface structure. The middle zone comprises a subhorizontal detachment (dip less than 10°) and an overlying nappe, with a total thickness of 15–18 km. The northern zone is the fold belt on the front of the surface structure, i.e., the Xishan anticline, which is expressed as a counter belt consisting of monoclinal strata in the shallow subsurface and an imbricate convex or compressive triangular zone in the deeper subsurface. Small earthquakes are confined to the low-angle detachment and overlying nappe. Within the root fault and frontal fold, earthquakes are relatively rare. By structural analogy, it is estimated that future major earthquakes may occur in the root portion of the structure. The exposed fault on the southern edge of the Chaiwopu basin has traces of activity in the Holocene, implying *M*7 events during that period. But the nappe of this structure (80–100 km long in the E-W direction) is smaller than that in the North Tianshan associated with the Manas *M*7.7 event in 1906 (some 200-km long in the E-W direction). Based on investigations of the Wangjiagou fault set, scarps of the Jiujiawan fault set, and an exploratory trench to identify paleoearthquakes (Fig. 7), we infer that the events of this nappe structure during the Holocene are around *M*7.3. Thus, the upper limit of future seismic risk for this seismogenic structure is *M*7.5.

The seismogenic model for thrust-fold earthquakes suggests that the frontier of a nappe structure is unable to produce *M*7 shocks. Thus the compressive triangular zone and convex structure below the Xishan uplift might suffer *M*6 earthquakes, with a maximum of *M*6.5. Events of such size cannot in general produce surface ruptures. The fault scarps seen along the Wangjiagou fault set and Jiujiawan fault set should be the deformation on the surface caused by compression that stemmed from the *M*7 earthquake at the root of the nappe and transmitted toward the north onto the Xishan uplift. In character, it is analogous to the earthquake fault caused by the 1906 Manas *M*7.7 event at

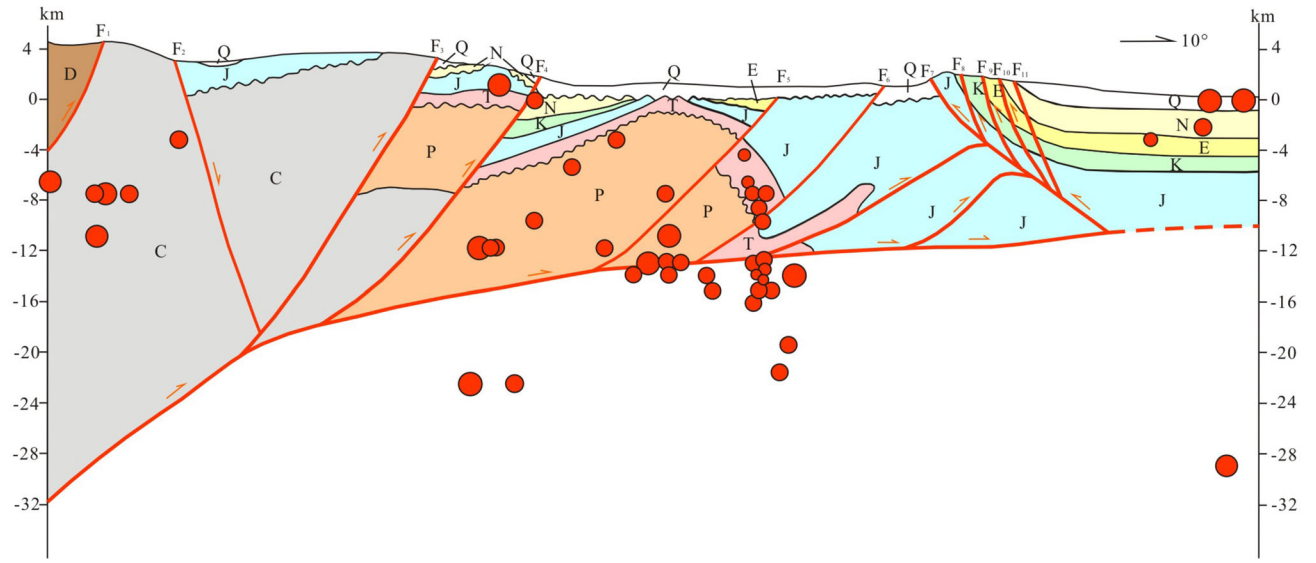

Fig. 6 Seismotectonic profile model in the west of Urumqi city. F_1-Houxia fault, F_2-Sijintian fault, F_3-Southern branch of the south margin fault of Chawopu basin, F_4-Northern branch of the south margin fault of Chawopu basin, F_5-North margin fault of Chawopu basin, F_6-Dapugou fault, F_7-Xishan fault, F_8-F_{10}-Wangjiagou fault group. *D*-limestone, calcareous sandstone, and andesite of Devonian; *C*-volcano tuff, silty mudstone, and valley-stone of Carboniferous; *P*-sandstone, *oil shale*, silty mudstone of Permian; *T*-mudstone, sandy mudstone, and stone Triassic; *J*-conglomerate, sandstone, mudstone, and coal seam of Jurassic; *K*-mudstone, sandstone and conglomerate of Cretaceous; *E*-mudstone and sandstone of Palaeogene; *N*-sandy conglomerate, sandstone and sandy mudstone of Neogene; *Q*-alluvial, and fluvial gravel and sand layers of Quaternary

the front of the range-frontal second row of anticlines. The source or epicenter is about 40 km from the seismic fault on the surface.

5.2 Bogda arc west flank seismogenic model

As defined by seismic profiles and geological data, this is also a thrust nappe structure like that in the North Tianshan. It comprises the root fault, middle detachment, and frontal compressive uplift zone. The root fault is probably just the Erdaogou fault, which is the boundary between the high and medium elevations where the Carboniferous System is thrust onto the Permian System (Fig. 8). Very probably, this fault was responsible for the *M*6.6 shock at Bogda, east of Urumqi city, in 1965. Previous studies have suggested that this fault has been active since the Holocene. Relocations of small earthquakes show a concentration of epicenters along the fault, but it terminates at the eastern edge of Urumqi city, so cannot generate a *M*7 shock in the study area.

The detachment nappe in the middle of the profile includes three imbricate thrust structures, of which the thrust in the south is the south-vergent (dipping 50°) Yamalik fault that thrusts the Permian onto the Mesozoic strata. Geological evidence shows that this fault has not been active in the study area since the late Pleistocene. In the east, up to the apex of the Bogda arc, it might have been active since the Pleistocene. Along the model profile (Fig. 8), small earthquakes occur near the Yamalik fault.

The Bagang-Shihua fault is exposed in the middle of the upper portion of the model profile (Fig. 8), and is comprised upper and lower flats and ramps. The lower flat lies in Permian oil-bearing shale and the upper flat in Jurassic coal strata. The flats dip at 10°–20° and ramps at 40°–50°, respectively, toward the south to exhibit a listric style. In addition, two north-vergent counter-thrust faults branch from the upper flat, i.e., the Wanyaogou and Baiyangnangou faults. Both these and the Bagang-Shihua fault have been active since the late Pleistocene, and jointly controlled the formation of the wedge-like Qidaowan anticline at the front.

In the north of the profile (Fig. 8), the Fukangnan thrust fault also has upper and lower flats and ramps. The dip angle of the flats is less than 10°, and they lie in the same strata as the aforementioned Bagang-Shihua fault. The Gumudi anticline is situated at the front of the Fukangnan fault, which has been active since the Holocene. In the south of the anticline, there is a counter-thrust fault, which is clear on the seismic profile from petroleum exploration. Below the Gumudi anticline, there are stack and compressive triangular structures controlled by imbricate thrust faults (Mitra 2002; Boyer and Elliott 1982), where there have recently been frequent small shocks.

For the three major thrust faults mentioned above, their active ages become younger from south to north, implying that the thrust nappe is spreading toward the north. They probably merge with the Erdaogou fault at the root of the

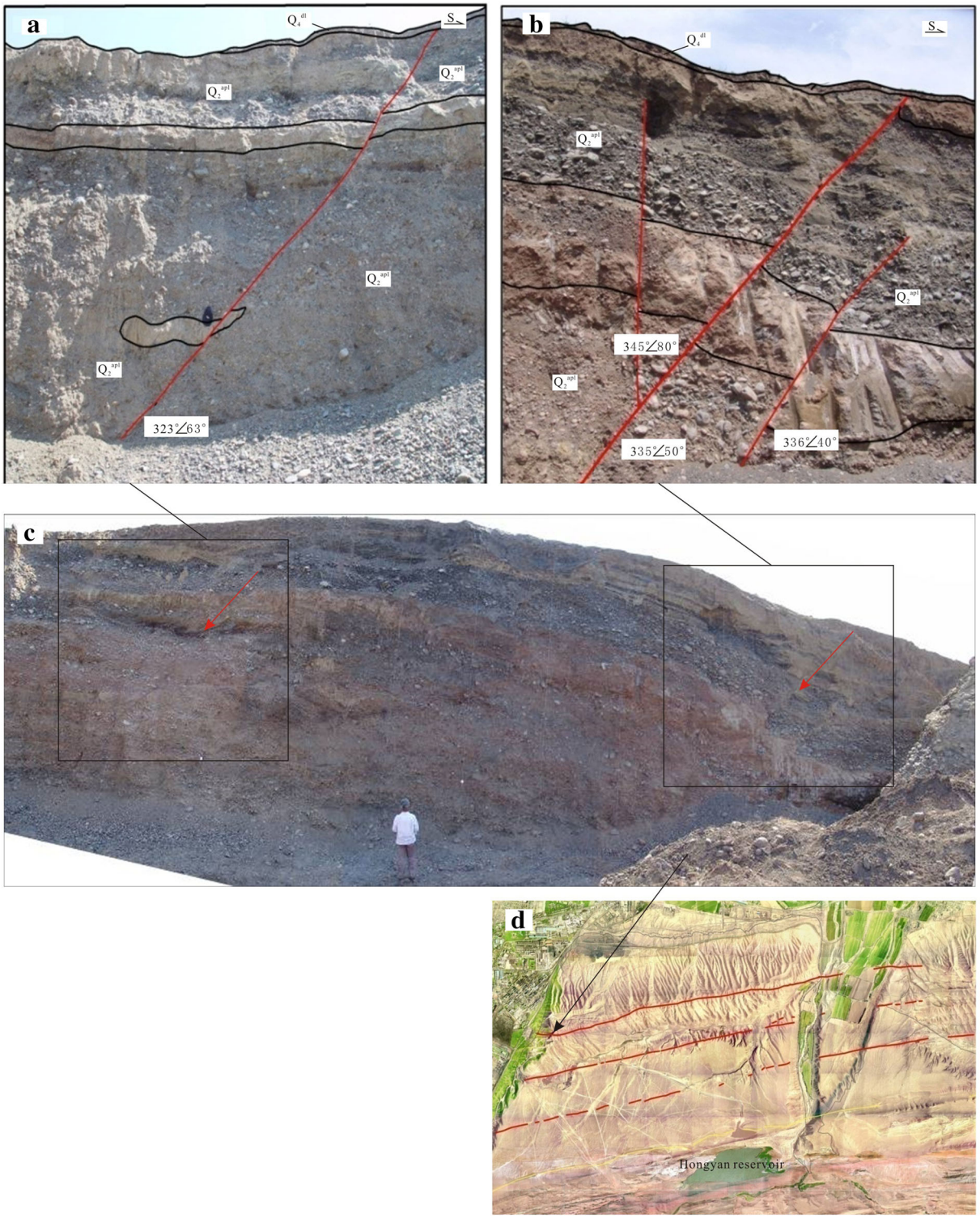

Fig. 7 The Wangjiagou fault group in Urumqi composed of four faults. Three of them on the north side were active during the Holocene. The picture at the *bottom* is an aerial picture. The fault landform can be clearly seen from it; from trench sections, the *middle* picture shows that the Quaternary stratigraphic section was offset by the Wangjiagou fault group; the pictures in the *upper left* and *upper right* panels show parts of the faults in trench sections

nappe structure. At present, the Fukangnan fault in the north and the Erdaogou fault in the south are active. The former is relatively shallower, capable of generating *M*6 but not *M*7 earthquakes and the latter lies at the end of the structure, also unable to produce *M*7 events. The maximum seismic risk of these two faults is *M*7.0. The other faults

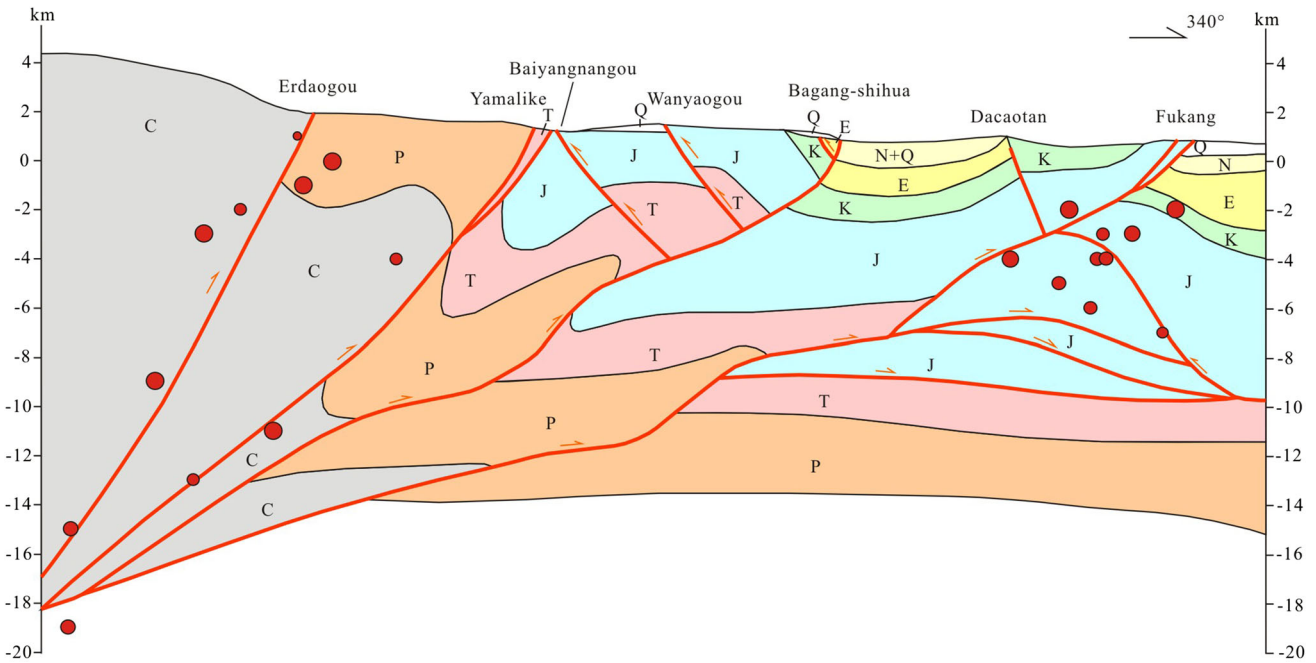

Fig. 8 Seismotectonic profile model in the east of Urumqi city (for location, see Fig. 1). *D*-limestone, calcareous sandstone and andesite of Devonian; *C*-volcano tuff, silty mudstone and valley-stone of Carboniferous; *P*-sandstone, oil shale, silty mudstone of Permian; *T*-mudstone, sandy mudstone and stone Triassic; *J*-conglomerate, sandstone, mudstone and coal seam of Jurassic; *K*-mudstone, sandstone and conglomerate of Cretaceous; *E*-mudstone and sandstone of Palaeogene; *N*-sandy conglomerate, sandstone and sandy mudstone of Neogene; *Q*-alluvial, and fluvial gravel and sand layers of Quaternary

that have not been active since the Holocene, such as the Wanyaogou, Baiyangnangou, Bagang-Shihua and Yamalik faults, might cause *M*6.5 shocks, slightly higher than the background value of *M*6.0 for the study region.

6 Discussion and conclusions

This work focuses on the seismotectonics of Urumqi city which lies in the frontal area of the North Tianshan Mountains. We have made a detailed analysis of seismogenic structures based on data from geological investigations of active faults, deep seismic soundings, and reflection profiles from petroleum exploration, as well as the relocation of small earthquakes.

The result shows that Urumqi city has two seismogenic structures, both of which are thrust nappes. One is the range-frontal thrust nappe in the North Tianshan in the west, and the other is the west flank of the Bogda arc in the east. The nappe system in the North Tianshan consists of the root thrust fault, middle detachment, and fold-uplift at the front. The faults at the root and upper portion of the frontal fold-uplift have been active since the Holocene. The detachment in the middle is characterized by spreading from south to north. Earthquakes of *M*7 magnitude occur near the root fault, and the fold-uplift at the front is capable of generating *M*6 shocks. The nappe structure in the Bogda arc has similar characteristics, where the Fukangnan fault and Erdaogou fault are active and capable of *M*6 events.

The two seismogenic models are based on information compiled from many sources, though they require further improvement. For instance, the seismogenic structure of the west flank of the Bogda arc is defined using the profile data from petroleum exploration which only extends to a shallow depth; thus a supplementary deep seismic sounding is required to clarify the model there. The accuracy, observational time and number of events are far from sufficient for precise relocation to reveal the relationship between seismic sources and deep structures. The possible maximum magnitude for future earthquake risk in the study area is merely a preliminary estimation and will be tested by more lines of evidence. Nonetheless, the models suggested in this paper have made some progress with respect to previous work and will be useful in the assessment of earthquake hazard in this region.

Acknowledgments This work is supported by Teachers Fund of China Earthquake Administration under Grant No. 20120101, National Natural Science Foundation of China under Grant No. 41372216, the State Special Project for International Cooperation on Science and Technology 2012DFR20440K02, the Fundamental Research Funds for the Central Universities under Grant No. ZY20120102.

References

Abdrakhmatov K, Aldazhanov S, Hager B, Hamburger M, Herring T, Kalabaev K, Makarov V, Molnar P, Panasyuk S, Prilepin M, Reilinger R, Sadybakasov I, Souter B, Trapeznikov Yu, Tsurkov V, Zubovich A (1996) Relatively recent construction of the Tian Shan inferred from GPS measurements of present-day crustal deformation rates. Nature 384(6608):450–453

Allen M, Vincent S, Wheeler P (1999) Late Cenozoic tectonics of the Kepingtage thrust zone: interactions of the Tien Shan and Tarim Basin, Northwest China. Tectonics 18(4):639–654

Avouac J, Tapponnier P, Bai M, You H, Wang G (1993) Active thrusting and folding in the northern Tien Shan and late Cenozoic rotation of the Tarim relative to Dzungaria and Kazakhstan. Geophys Res 98(4):6755–6804

Boyer S, Elliott D (1982) Thrust systems. AAPG Bull 66:1196–1230

Burbank D, Anderson R (2001) Tectonic geomorphology. Blackwell Science, Oxford, p 105

Burbank D, McLean J, Bullen M, Abdrakhmatov K, Miller M (1999) Thrust-belt partitioning of intermontane basins by basement folding, Tien Shan, Kyrgyzstan. Basin Res 11:75–92

Burchfiel B, Brown E, Deng Q, Feng X, Li J (1999) Crustal shortening on the margins of the Tien Shan, Xinjiang, China. Int Geol Rev 41(8):665–700

Chen Z, Zhu S, Li Q, Chen D, Liu A, Chen B (2012) Study of interval velocity calculating and its application based on improved Dix formulas. Sci Technol Eng 12(30):7840–7845 **(in Chinese with English abstract)**

Deng Q, Feng X, Zhang P, Xu X, Yang X, Peng S, Li J (2000) Active Tectonics of Tianshan. Seismological Press, Beijing, pp 1–399 **(in Chinese with English abstract)**

Fu B, Lin A, Kano K, Maruyama T, Guo J (2003) Quaternary folding of the eastern Tian Shan, northwest China. Tectonophysics 369:79–101

Ghose S, Hamburger M, Ammon C (1998) Source parameters of moderatesized earthquakes in the Tien Shan, Central Asia from regional moment tensor inversion. Geophys Res Lett 25(16):3181–3184

Khain EV, Bikova EV, Salnikova EB, Kroner A, Gibsher A, Didenko A, Degtyarev K, Fedotova A (2003) The Palaeo-Asian ocean in the neoproterozoic and early palaeozoic: new geochronologic data and palaeotectonic reconstructions. Precambr Res 122:329–358

Kuang J, Qi X (2006) The structural characteristics and oil-gas explorative direction Junggar Foreland Basin. Xinjiang Pet Geol 27(1):5–6 **(in Chinese with English abstract)**

Li X (2003) The application of several explaining techniques in complex, structure in the south of Jungar Basin. J Xinjiang Pet 15(1):5–10 **(in Chinese with English abstract)**

Li X, Wang B, Chen Y (2006) The fracture patterns and oil-controlled process in Piedmo Margin of Junggar Basin. Xinjiang Pet Geol 27(3):285–287 **(in Chinese with English abstract)**

Li J, Chen G, Wei W, Zainnula P, Wang X, Liu D, Li G, Fang W, Chen S, Sun X (2016) Study on characteristics of present-day tectonics movement of typical faults in northern Tianshan Mountain. Acta Seismol Sin, in press **(in Chinese with English abstract)**

Liu H, Liang H, Cai L et al (1994) Evolution and structural style of Tianshan and adjacent Basins, northwestern China. J China Univ Geosci 5(1):46–54

Liu B, Shen J, Zhang X, Chen Y, Fang S, Song H, Feng S, Zhao C (2007) The crust structures and tectonics of Urumqi depression revealed by deep seismic reflection profile in the northern margin of Tianshan Mountains. Chin J Geophys 150(5):1464–1472 **(in Chinese with English abstract)**

Mitra S (2002) Fold-accommodation faults. AAPG Bull 86:671–693

Ran Y, Chen L, Shen J, Li J, Gong H (2007) Xishan fault group near Urumqi city and paleoearthquake identification on reverse fault. Seismol Geol 29(2):219–233 **(in Chinese with English abstract)**

Song H, Shen J, Xiang Z, Li J, Rou J (2009) The Active Fault Detecting and Seismic Risk Assessment in Urumuqi City. Seismological Press, pp 83–99 **(in Chinese)**

Stein R (1984) Coalinga's caveat. EOS, Am Geophys Union Trans 65:791–795

Stein R, Yeats RS (1989) Hidden earthquakes. Sci Am 260(6):48–57

Wang Y, Shen J (2000) The basic features of the active tectonics in the northern foothill of Tianshan Mountain, China. Xinjiang Geol 18(3):203–210 **(in Chinese with English abstract)**

Wang C, Lou H, Wei X, Wu Q (2001) Crustal structure in northern margin of Tian-Shan Mountains and seismotectonics of 1906 Manas earthquake. Acta Seismol Sin 14(5):491–502

Wu Z, Guo F (1991) Second discussion on the Bogda nappe tectonics and its oil-gas accumulation. Xinjiang Geol 9(1):40–49 **(in Chinese)**

Wu C, Shen J, Shi J, Li J, Xiang Z (2011) Surface deformation of the WangJiaGou fault set in urumuqi and the safety distance from it. Seismol Geol 33(1):56–66 **(in Chinese with English abstract)**

Wu C, Wu G, Shen J, Dai X, Chen J, Song H (2016) Late Quaternary tectonic activity and crustal shortening rate of the Bogda Mountain area, eastern Tian Shan, China. J Asian Earth Sci 119:20–29

Xi Li, Liu L, Chen W (2004) The analysis of structural model of Gumudi Anticline in southern margin of Junggar Basin. Xinjiang Pet Geol 25(2):141–1420 **(in Chinese)**

Yang S, Li J, Wang Q (2008) The deformation pattern and fault rate in the Tianshan Mountains inferred form GPS observations. Sci China (Ser D) 51(8):1064–1080

Yeats R (1986) Active faults related to folding in active tectonics. National Academy Press, Washington

Zhang P, Deng Q, Xu X, Peng S, Yang X, Feng X, Zhao R, Li J (1994) Blind thrust, folding earthquake, and the 1906 Manas earthquake, Xinjiang. Seismol Geol 16(3):193–204 **(in Chinese with English abstract)**

Zhang P, Deng Q, Yang X, Peng SZ, Xu XW, Feng XY (1996) Late Cenozoic tectonic deformation and mechanism along the Tian-shan Mountain, North Western China. Earthq Res China 12(2):127–140 **(in Chinese with English abstract)**